NEOPLASIA
www.neoplasia.com

Volume 15 Number 4 April 2013 pp. 421–434 421

γ-Catenin at Adherens Junctions: Mechanism and Biologic Implications in Hepatocellular Cancer after β-Catenin Knockdown[1,2]

Emily Diane Wickline*, Yu Du*, Donna B. Stolz†, Michael Kahn‡ and Satdarshan P. S. Monga*,§

*Department of Pathology, University of Pittsburgh School of Medicine, Pittsburgh, PA; †Department of Cell Biology, University of Pittsburgh School of Medicine, Pittsburgh, PA; ‡Department of Molecular Pharmacology and Toxicology, Center for Molecular Pathways and Drug Discovery, University of Southern California, Los Angeles, CA; §Department of Medicine, University of Pittsburgh School of Medicine, Pittsburgh, PA

Abstract

β-Catenin is important in liver homeostasis as a part of Wnt signaling and adherens junctions (AJs), while its aberrant activation is observed in hepatocellular carcinoma (HCC). We have reported hepatocyte-specific β-catenin knockout (KO) mice to lack adhesive defects as γ-catenin compensated at AJ. Because γ-catenin is a desmosomal protein, we asked if its increase in KO might deregulate desmosomes. No changes in desmosomal proteins or ultrastructure other than increased plakophilin-3 were observed. To further elucidate the role and regulation of γ-catenin, we contemplate an *in vitro* model and show γ-catenin increase in HCC cells upon β-catenin knockdown (KD). Here, γ-catenin is unable to rescue β-catenin/T cell factor (TCF) reporter activity; however, it sufficiently compensates at AJs as assessed by scratch wound assay, centrifugal assay for cell adhesion (CAFCA), and hanging drop assays. γ-Catenin increase is observed only after β-catenin protein decrease and not after blockade of its transactivation. γ-Catenin increase is associated with enhanced serine/threonine phosphorylation and abrogated by protein kinase A (PKA) inhibition. In fact, several PKA-binding sites were detected in γ-catenin by *in silico* analysis. Intriguingly γ-catenin KD led to increased β-catenin levels and transactivation. Thus, γ-catenin compensates for β-catenin loss at AJ without affecting desmosomes but is unable to fulfill functions in Wnt signaling. γ-Catenin stabilization after β-catenin loss is brought about by PKA. Catenin-sensing mechanism may depend on absolute β-catenin levels and not its activity. Anti–β-catenin therapies for HCC affecting total β-catenin may target aberrant Wnt signaling without negatively impacting intercellular adhesion, provided mechanisms leading to γ-catenin stabilization are spared.

Neoplasia (2013) 15, 421–434

Introduction

Hepatocellular carcinoma (HCC) is the fifth most common cancer worldwide, and the severity of the disease has resulted in it becoming the third leading cause of cancer-related deaths worldwide [1,2]. Only about one-third of HCCs are curable by surgical resection, and the current treatments for the majority of HCC cases involve non-targeted palliative care, such as systemic chemotherapies [3]. Therefore, understanding and treating this disease at a cellular and molecular level becomes imperative to relieve this major health burden. Pathologically, an abnormal distribution of the armadillo family protein β-catenin has been described in up to 90% of HCC cases [4–6]. Of these, β-catenin

Address all correspondence to: Satdarshan P. S. Monga, MD, Professor of Pathology and Medicine, University of Pittsburgh School of Medicine, 200 Lothrop Street S-422 BST, Pittsburgh, PA 15261. E-mail: smonga@pitt.edu

[1]This study was funded by National Institutes of Health grants 1R01DK62277 and 1R01CA124414 to S.P.S.M. and also partially funded by Endowed Research Chair to S.P.S.M.

[2]This article refers to supplementary materials, which are designated by Tables W1 and W2 and are available online at www.neoplasia.com.

Received 11 December 2012; Revised 29 January 2013; Accepted 30 January 2013

DOI 10.1593/neo.122098

gene (*CTNNB1*) mutations have been reported in 30% [7]. On the basis of the many roles of β-catenin in HCC biology, it has been discussed as a potential therapeutic target. Our laboratory and others have recently proposed a number of unique anti–β-catenin therapies for the treatment of HCC [8–11].

β-Catenin is an essential component of Wnt signaling pathway [12]. Wnt/β-catenin is important in liver homeostasis and regulates zonation, development, metabolism, proliferation, and regeneration [13]. Additionally, β-catenin is also a key component of cell-cell adhesions at the adherens junctions (AJs), where it links the transmembrane protein E-cadherin to the actin cytoskeleton. Despite β-catenin's critical role in the liver, we previously published that a hepatocyte-specific β-catenin knockout (KO) mouse was viable and had no overt adhesive defect [14]. We also showed that with loss of hepatic β-catenin there is an increase of γ-catenin (plakoglobin) over the wild type (WT), specifically at the AJ. γ-Catenin is a major protein in cell-cell adhesion at the desmosomes, where it also links transmembrane cadherins (desmogleins and desmocollins) to intermediate filaments of the actin cytoskeleton. γ-Catenin is found in the armadillo family of proteins along with β-catenin, shares nearly an 80% homology to β-catenin, and has a nearly identical interaction with E-cadherin [15]. There have also been reports that γ-catenin has potential nuclear functions through the Wnt signaling pathway in β-catenin–null cell lines [16,17].

Cell-cell junctions are essential to proper hepatocyte functionality. Hepatocyte junctions regulate the flow of molecules between hepatocytes, help maintain cellular polarity, and create barriers within the liver. Compromised barriers occur in liver pathologies, such as cholestasis [18], biliary cirrhosis [19], and HCC. Studies have shown that the levels of AJ and desmosomal protein expression correlate with the differentiation status of clinical HCC cases. In poorly differentiated HCC cases, more than 50% of tumor cells and nearly 100% of cancer cells no longer expresses AJ and desmosomal components [20]. Additionally, HCC patients with underexpression of γ-catenin have a poor survival [21]. Therefore, dysregulated junctions are observed in HCC.

In the present study, we demonstrate that the *in vivo* compensation of γ-catenin in β-catenin KO mice does not come at the expense of desmosomes. We show in an *in vitro* model that γ-catenin alleviates β-catenin loss at AJ to maintain cell-cell adhesion but is unable to fulfill its role in the canonical Wnt signaling. Lastly, we identify the mechanism of γ-catenin stabilization to be serine/threonine phosphorylation induced by protein kinase A (PKA). Thus, we show that β-catenin–lowering agents may be a viable option for HCC treatment, provided γ-catenin stabilization mechanisms are spared.

Materials and Methods

Animals

All animal studies were approved by the University of Pittsburgh Institutional Animal Care and Use Committee office. Homozygous floxed β-catenin mice (C57BL/6 strain) and albumin-cre transgenic mice were bred as previously described [14]. Mice with genotype *CTNNB1*$^{lox/lox}$; Alb-Cre$^{+/-}$ are referred to as KOs. Littermates with floxed β-catenin genotypes were used as WT controls. Livers from age- and sex-matched 60- to 120-day-old KO and WT ($n < 4$) were used, unless otherwise noted.

Cell Lines and Treatments

Hep3B and HepG2 human HCC cell lines were obtained from the American Type Culture Collection (Manassas, VA). Cells were cultured in Eagle's minimal essential medium (EMEM) supplemented with 10% vol/vol FBS at 37°C in a humidified 5% carbon dioxide atmosphere. For transient transfection, the cells were plated in six-well plates and grown to 60% to 80% confluence, followed by serum starvation for 4 to 16 hours. For siRNA KD, the cells were transfected using Lipofectamine 2000 (Life Technologies, Grand Island, NY) and a total siRNA concentration of 75 nM and/or DNA concentration of 500 ng in Opti-MEM I Media (Life Technologies) for 24 to 72 hours as per the manufacturer's instructions. Human γ-catenin (*JUP*), prevalidated β-catenin (*CTNNB1*), and scrambled Negative Control 2 Silencer Select siRNAs were purchased from Ambion (Grand Island, NY). Additionally, *CTNNB1* (ISIS102708) or control antisense oligonucleotides (ASOs; ISIS Pharmaceuticals Inc, Carlsbad, CA) were used for transient transfections at a concentration of 50 nM for 24, 48, or 72 hours as previously published [22]. Small molecule inhibitor of β-catenin nuclear activity, ICG-001, was used for cell treatments at 10 mM as previously published [8]. All experiments were performed in triplicate.

Hep3B cells were also treated with the phosphatase inhibitor okadaic acid (OA) (Santa Cruz Biotechnology, Santa Cruz, CA) at 25 and 10 nM, as previously published, for 3 hours [23]. After transfecting Hep3B cells for 21 or 45 hours with β-catenin or control siRNA against β-catenin, serine/threonine kinase inhibitors, purchased from Calbiochem (Billerica, MA), were administered for 3 hours at the following concentrations: H-89 at 20 μM [24], protein kinase G (PKG) inhibitor (RKRARKE) at 200 μM [25], bisindolylmaleimide I at 1 μM [26], KN-93 at 5 μM [27], ML-7 at 30 μM [28], staurosporine at 1 μM [29]. Cells were washed and used for whole-cell lysate (WCL) and Western blot (WB).

β-Catenin/TCF Transcription Reporter Assay

Cells were transiently transfected with the reporter construct TOPflash (Upstate, Lake Placid, NY), which has three copies of T cell factor (TCF)/LEF sites upstream of a thymidine kinase promoter and the firefly luciferase gene. Cells were co-transfected with Renilla luciferase to control for transfection efficiency. This reporter system has been successfully used to detect both β- and γ-catenin–dependent Wnt signaling [16,30]. Luciferase assays were performed using Dual-Luciferase Reporter Assay System (Promega, Madison, WI). Average relative light units from triplicate experiments were compared for statistical significance by Student's *t* test.

Protein Extraction

WCLs were obtained using radioimmunoprecipitation assay buffer containing fresh protease and phosphatase inhibitor cocktails (Sigma, St Louis, MO) as described previously [14]. Cytoskeleton-associated proteins were also extracted as described previously [31] to obtain Triton X-100–insoluble (I) or cytoskeletal-associated lysates (CALs). Nuclear lysates were extracted using NE-PER Nuclear and Cytoplasmic Extraction Kit as per the manufacturer's instructions (Pierce, Rockford, IL). Protein assays were performed using BCA protein assays (Pierce).

Western Blot

A total of 10 to 20 μg of protein was resolved on Tris-HCl precast gels (Bio-Rad Laboratories, Hercules, CA) by sodium dodecyl sulfate–polyacrylamide gel electrophoresis analysis using the Mini-PROTEAN 3 Electrophoresis Module Assembly (Bio-Rad Laboratories). The resolved proteins were transferred to polyvinylidene difluoride membranes and

the signal was detected by SuperSignal West Pico Chemiluminescent Substrate (Pierce). HRP-conjugated secondary antibodies were purchased from Millipore (Billerica, MA). Whenever necessary, WBs were quantified using ImageJ software (National Institutes of Health, Bethesda, MD). A complete list of primary antibodies and dilutions is provided in Table W1.

Immunoprecipitation

Co-precipitation studies were performed with 200 to 500 μg of WCL or CAL as described elsewhere [31]. Antibodies used for immunoprecipitation (IP) were rabbit anti–γ-catenin (Cell Signaling Technology, Danvers, MA), rabbit anti–E-cadherin (Santa Cruz Biotechnology), or goat β-catenin–conjugated A/G agarose beads (Santa Cruz Biotechnology).

Immunofluorescence

Staining was performed using goat anti–γ-catenin (sc-30997) or rabbit anti–β-catenin (sc-7199; Santa Cruz Biotechnology), primary antibodies, and Alexa 488–conjugated donkey anti-goat and Alexa 555–conjugated donkey anti-rabbit (Life Technologies) secondary antibodies, as described elsewhere [32]. Sections were counterstained with 4',6-diamidino-2-phenylindole (DAPI) and imaged with Olympus 1000 Confocal Microscope with Fluoview 1.7A software (Center Valley, PA).

Transmission Electron Microscopy

Liver tissue was fixed with 2.5% glutaraldehyde in phosphate-buffered saline (PBS) by perfusion through the inferior vena cava. Transmission electron microscopy (TEM) was performed as described previously [33]. Briefly, after fixation and sectioning, grids were hand stained with 2% uranyl acetate in 50% methanol for 10 minutes and 1% lead citrate for 7 minutes. Digital TEM images were taken with JEOL JEM-1011 Transmission Electron Microscope (Peabody, MA) at 80.0 kV. Quantitative analysis of junctions was done with MetaMorph Software (Molecular Devices, Sunnyvale, CA).

Microarray Analysis

Livers from three KO and WT were used for Affymetrix (Santa Clara, CA) gene array analysis as previously published [14]. The signals from KO and WT livers were compared and presented as fold change.

Real-Time Polymerase Chain Reaction

RNA was extracted from treated Hep3B cells using TRIzol (Life Technologies) and was DNAse-treated using the TURBO DNAse Kit (Ambion) as per the manufacturer's instructions. The RNA was used for real-time polymerase chain reaction (PCR) analysis as described elsewhere [34]. Comparative delta-delta Ct (DDCT) method was used for analysis of the data, and calculations were made without the StepOne software (Applied Biosystems, Grand Island, NY). Real-time PCR primer sequences are available in Table W2.

Proliferation Assay ([^{3}H]Thymidine Incorporation)

Proliferation analyses were performed as previously described [35]. Briefly, 24 hours after siRNA transfection in Hep3B cells, [^{3}H]thymidine (2.5 mCi/ml) was added to culture media. The cells were cultured for [^{3}H]thymidine incorporation for an additional 24 to 48 hours. The cells were then washed with 5% ice-cold trichloroacetic acid (TCA) and lysed with 0.33 M NaOH. Aliquots diluted in scintillation fluid were used to determine [^{3}H]thymidine incorporation on a Beckman Scintillation counter (Brea, CA). Average counts per minute from triplicate experiments were compared for statistical significance by Student's *t* test.

Scratch Wound Assay

Wound-healing assays were performed as previously described [36]. Briefly, cells were grown as a confluent monolayer and transfected for 24 hours, and a wound was made using a p10 pipette tip. During the assay, cells were cultured in 0.5% EMEM to decrease the influence of cell proliferation. Cells were imaged periodically for 24 additional hours until the wound fronts began to merge. The wounds were imaged at four different locations for each time point using phase-contrast filters at 5× magnification on an Axioskop 40 (Zeiss, Thornwood, NY) inverted brightfield microscope, and the cell-free area of the scratches was quantified at each time point using ImageJ software (National Institutes of Health). Percentage of wound closure from triplicate experiments was compared for statistical significance by Student's *t* test.

Cell-Cell Adhesion Assays

CAFCA was performed as previously described [36]. Briefly, transfected cells were prelabeled with CellTracker Green CMFDA (Life Technologies) for 15 minutes at 37°C, non-enzymatically dissociated from the monolayers using a 1:200 dilution of 500 mM EGTA and 500 mM EDTA in calcium and magnesium-free Hank's balanced salt solution, and resuspended in 10% EMEM to be replated on unlabeled confluent monolayer of non-transfected cells cultured on collagen-coated plates. After 30 minutes, the wells were washed once with PBS to remove cells that did not attach, and fluorescence intensity of labeled cells was quantified using a plate fluorometer at 495/515 nm. The inverted plate was centrifuged at 375*g* in airtight chamber filled with warm culture media for 10 minutes. Cells were washed and fluorescence intensity of the remaining labeled cells was measured. A value of 100% attachment was assigned to the fluorescent measurement recorded for each well before centrifuging the plate, and experimental data were expressed as a percentage of cells lost *versus* the initial 495/515 nm reading. Percentage of cells lost from triplicate experiments was compared for statistical significance by Student's *t* test.

Hanging drop assay was performed as described previously [37]. Briefly, treated cells were removed from their monolayer using trypsin and counted. The cells were resuspended in 2% EMEM at a concentration of 2.5×10^5 cells/ml, and 20 μl of drops containing 5000 cells/drop was pipetted onto the inner surface of a 10-cm^2 dish lid. The bottom of the petri dish was filled with 8 ml of PBS to prevent evaporation of the drops. The lid was placed back on the dish so that the drops of cells were hanging from the lid, and the cells were incubated for 20 hours at 37°C in a humidified 5% carbon dioxide atmosphere. Some drops were pipetted up and down 20 times to assess dissociation of cell colonies as a measurement of cadherin-mediated cell adhesion activity. Coverslips were placed over the drops, and images were taken using phase-contrast filters at 5× magnification on an Axioskop 40 (Zeiss) inverted brightfield microscope. Experiments were performed in triplicate ($n > 5$).

Statistics

Student's *t* test was performed using Microsoft Excel 2010 (Microsoft, Redmond, WA) to assess statistical significance for a minimum of three different data points per experiment. Unless otherwise noted,

significance was measured relative to control or siNegative treatments. A *P* value of less than .01 was considered to be significant. Bar graphs were made for each data set, and representative data are presented with SDs of the mean indicated with error bars.

Results

β- and γ-Catenins Are Mutually Exclusive at Hepatocyte Membranes

It has been recently reported that the albumin-Cre/Lox system of knocking out genes in hepatocytes may sometimes be "leaky" especially after about 6 months of age, causing some repopulation of KO livers with β-catenin–positive hepatocytes [38,39]. We used this anomaly as a proof of concept. We performed immunofluorescence (IF) staining on liver sections of an 8-month-old KO mice (on regular chow) to assess the localization of β- and γ-catenins at the membrane of hepatocytes. We previously reported that KO livers had an increase in γ-catenin co-localization with E-cadherin at the AJ [31]. Here, we see that β-catenin (red) and γ-catenin (green) appear to be mutually exclusive at the hepatocyte membranes, with no co-localization (Figure 1*A*). Analysis of the γ-catenin localization in the β-catenin–positive nodule shows a desmosomal-like staining pattern, while γ-catenin localization in the remainder of the KO liver section has an AJ-like staining pattern (Figure 1*A*, *inset*, green channel).

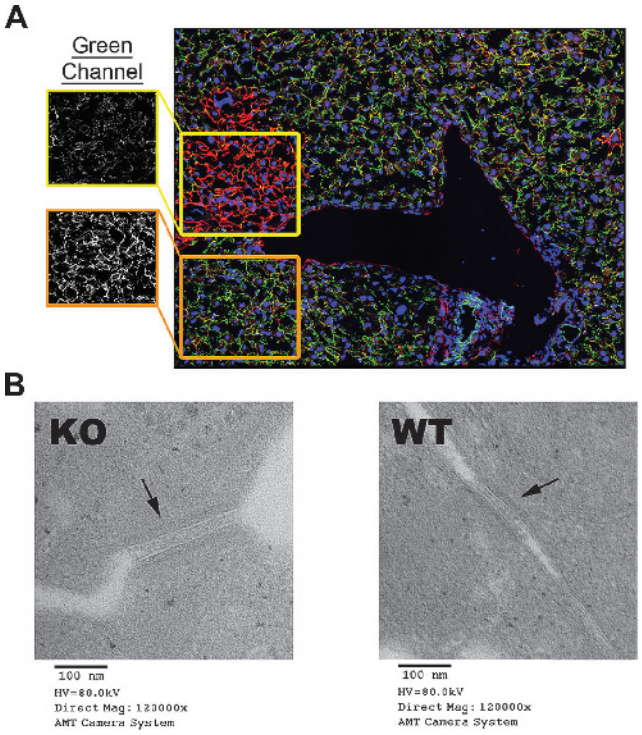

Figure 1. Assessment of AJs and desmosomes in β-catenin KO and WT livers. (A) Membranous γ-catenin (green) and β-catenin (red) are mutually exclusive at the cell membranes/AJ in β-catenin of hepatocytes in β-catenin KO livers that become repopulated with β-catenin–positive hepatocytes at elderly ages as shown by representative double IF images of fixed liver sections. Boxes show the staining pattern of γ-catenin (green channel) in β-catenin–positive and β-catenin–negative sections of the KO liver. (B) TEM of β-catenin KO and WT livers shows the presence of desmosomes (arrows). The intercellular distance between hepatocytes connected by desmosomes is not significantly different (mean distances: KO = 27.4 nm, WT = 25.1 nm; $P > .10$).

Table 1. Changes in Desmosomal mRNA Expression in β-Catenin KO in Microarray.

Gene/Protein	Cell-Cell Junction	Change in KO *versus* WT
Dsc-2	Desmosome	+2.2
Dsc-3*	Desmosome	+3.8
Pkp3	Desmosome	−3.7

*Not normally in the liver [20].

The Increase of γ-Catenin with β-Catenin Loss Is Not at the Expense of the Hepatic Desmosomes

γ-Catenin is able to compensate for β-catenin loss at the AJ by binding to E-cadherin [31,37,40–45]. This increase in γ-catenin is not transcriptional and may be a result of posttranslational stabilization [31,41,46]. However, γ-catenin is primarily a desmosomal protein, so is this compensation at the cost of desmosomal integrity? Initially, we used TEM to compare desmosome ultrastructure in KO and WT livers. We see recognizable desmosomes in both KO and WT (Figure 1*B*). Further analysis revealed no significant difference in intercellular distances at the point of desmosomal adhesions, with mean distances of 27.4 nm in the KOs and 25.1 nm in the WTs ($P > .10$).

Next, to investigate gene expression changes in desmosomal components, we analyzed microarray data from KO and WT livers [14]. KO livers showed altered expression of desmocollin-2 (Dsc-2; +2.2-fold), Dsc-3 (+3.8-fold), and plakophilin-3 (Pkp3, −3.7-fold; Table 1). Interestingly, Dsc-3 has never been shown to be present in the desmosomes of the livers, but we see a robust increase in mRNA expression in the KO livers [20].

Since changes in mRNA levels do not always correspond to overall protein levels, especially with catenins and cadherins [31], we wanted to further analyze the protein expression of liver-specific desmosomal proteins [47]. We analyzed soluble (S) and insoluble (I) CALs of β-catenin KO and WT livers for desmosomal protein expression by WBs (Figure 2*A*). β-Catenin KO livers show more soluble and insoluble γ-catenin than WTs by WBs (Figure 2*B*). We evaluated the levels of desmoplakin I and II (DPI/II), desmoglein-1 (Dsg1), Dsg2, Dsg3, Dsg4, Dsc-2, Pkp2, and Pkp3 (Figure 2*A*). There was no change in overall protein levels, despite changes in some mRNA levels (Table 1); interestingly, the protein Pkp3 is upregulated in S and I fractions (Figure 2*A*), despite a −3.7-fold decrease in mRNA expression (Table 2).

Next, we assessed if there was a change in the desmosomal protein association with γ-catenin. By IP, we show lack of any change in DPI/II, Dsg1, Dsg2 (data not shown), and Dsg4 association with γ-catenin between KO and WT livers in I fraction (Figure 2*C*) and S fraction lysates (data not shown). In summary, the lack of ultrastructural changes along with minimal changes in various desmosomal proteins and lack of changes in γ-catenin's interactions with various desmosomal proteins supports the notion that changes γ-catenin increase due to β-catenin loss is not at the expense of desmosomes.

No Qualitative Changes in Pkp3 with β-Catenin Loss

Next, we wanted to address if the species of Pkp3 that increased with β-catenin loss had different binding partners, which affects its trafficking in the cytoplasm. It was recently published that a complex of γ-catenin, E-cadherin, and Pkp3 is required to initiate desmosome formation [48]. Since both γ-catenin and Pkp3 are known binding

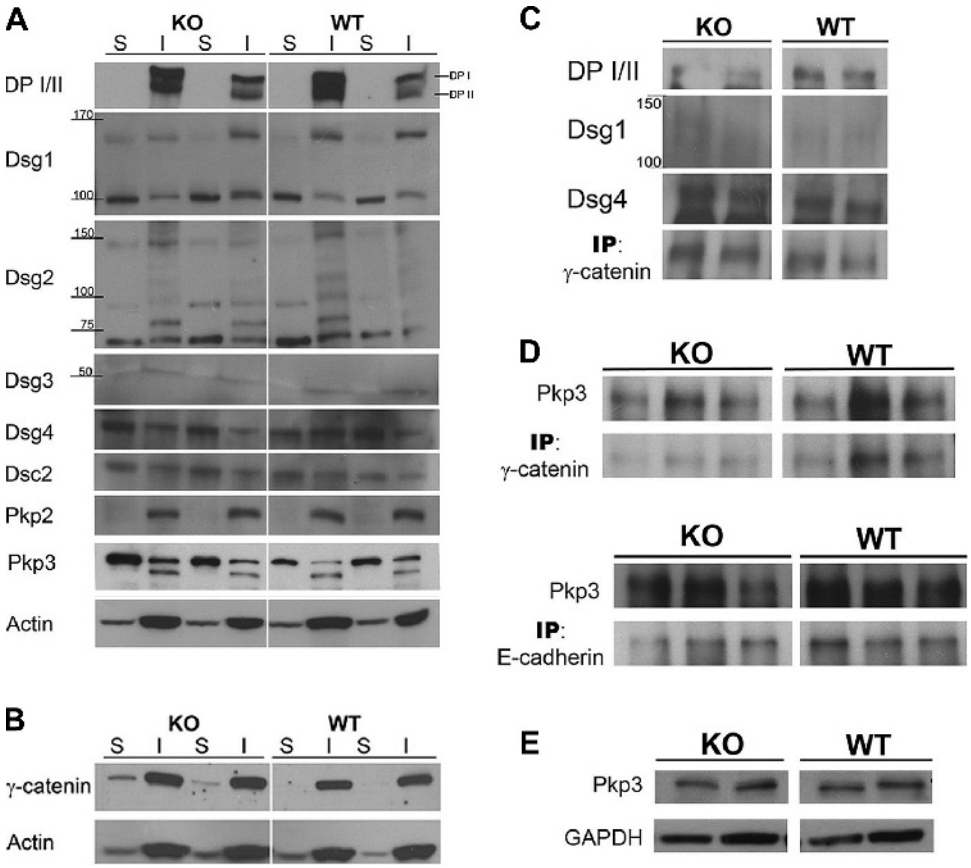

Figure 2. β-Catenin KO mouse livers show no changes in desmosomal proteins, except Pkp3. (A) β-Catenin KO livers have no apparent changes in most desmosomal protein levels in Triton X-100–soluble (S) and Triton X-100–insoluble/cytoskeleton-associated lysates (I) through WBs, despite mRNA changes (Table 1): DPI (250 kDa), DPII (210 kDa), Dsg1 (150 kDa), Dsg2 (59–150 kDa), Dsg3 (55–130 kDa), Dsg4 (100–115 kDa), Dsc2 (110 kDa), and Pkp2 (100 kDa). However, Pkp3 (87 kDa) is slightly increased in KO livers in both soluble (S) and insoluble (I) CAL fractions over WT age- and sex-matched liver lysates. (B) β-Catenin KO livers show more soluble and insoluble γ-catenin (83 kDa) than WTs by WBs. WB for actin (42 kDa) verifies comparable loading. (C) Representative IPs of γ-catenin in insoluble CAL fraction show no apparent changes in desmosomal protein associations with γ-catenin in β-catenin KO and WT livers. (D) Pkp3 co-precipitates with γ-catenin (upper panel) and E-cadherin (lower panel) equally in the soluble CAL fractions of KO and WT livers. (E) Nuclear lysates show that Pkp3 protein levels are similar between KO and WT livers.

partners, and both were increased with β-catenin loss, we investigated if these proteins associated more readily in the KO livers, possibly contributing to their mutual stabilization. IP studies show that Pkp3 binding to both E-cadherin and γ-catenin was observed in the S and I (not shown) CAL fractions, but there was no change in Pkp3 association with β-catenin loss (Figure 2*D*). To further investigate the possible reason for the increase in Pkp3 levels with β-catenin loss, we wanted to see if the increase Pkp3 levels lead to increased nuclear Pkp3, since it has been shown that Pkp3 has the potential to have nuclear functions [49]. Here, we show that there is nuclear Pkp3 in the KO and WT livers, but there is no difference with β-catenin loss (Figure 2*E*). Therefore, the changes in Pkp3 levels with β-catenin loss cannot be explained by changes in cytoplasmic binding partners or with nuclear localization.

β-Catenin Knockdown in Hep3B Human Hepatoma Cells Induces γ-Cateninto Replicate β-Catenin KO In Vivo

We next investigate if changes in γ-catenin due to chronic β-catenin loss *in vivo* in hepatocytes can also occur acutely *in vitro*. siRNA-mediated acute knockdown (KD) of β-catenin increases γ-catenin protein levels *in vitro* in Hep3B, a human HCC cell line (Figure 3*A*). As in the *in vivo* model, siRNA KD of β-catenin induced E-cadherin–γ-catenin co-precipitation in the Hep3B cells compared to the scrambled siRNA-transfected cells (Figure 3*B*). Reciprocally, γ-catenin co-precipitates to a greater extent with E-cadherin upon β-catenin KD in Hep3B cells (Figure 3*B*, *lower panel*). Hence, the *in vitro* model using Hep3B cells accurately replicates key observations seen in hepatocyte-specific KO mice.

To verify that the observed increase in γ-catenin in Hep3B cells after siRNA-mediated β-catenin KD is not cell-specific or reagent-specific, we next employed ASO to KD β-catenin in not only Hep3B but also in HepG2 cells, which carry a monoallelic deletion of exon-3 in *CTNNB1* gene. ASO against β-catenin decreased its protein levels and concomitantly increased the levels of γ-catenin (Figure 3*C*). These data demonstrate that an increase in γ-catenin occurs with β-catenin decrease regardless of the method of KD, cell line used, or presence of full-length or mutated β-catenin in a hepatoma cell.

KD of β-Catenin Levels but Not Decrease in Its Activity Induces γ-Catenin Increase in Hepatoma Cells

We next asked if the increase in γ-catenin occurs secondary to decrease in β-catenin levels, its activity, or both. We used a small molecule

inhibitor of β-catenin's nuclear functions, ICG-001, that binds to the co-activator CREB-binding protein, a known histone acetyltransferase, thereby disrupting the CREB-binding protein–β-catenin interactions to downregulate β-catenin/TCF4–dependent target gene expression [8]. Indeed, treatment of Hep3B cells with ICG-001 led to decrease in β-catenin target cyclin D1 (Figure 3*D*) and TOPflash luciferase reporter activity (data not shown). However, unlike siRNA or ASO, ICG-001 does not decrease overall β-catenin protein expression (Figure 3*D*). Intriguingly, ICG-001 treatment did not lead to any increase in γ-catenin in these cells, and if at all, a modest decrease was evident in these cells (Figure 3*D*). Thus, these data suggest that cells sense a decrease in total β-catenin protein and not its activity to trigger an increase in γ-catenin protein.

γ-Catenin Stabilization after β-Catenin KD Occurs through PKA and PKG-Mediated Serine/Threonine Phosphorylation

Next, we assess the mechanism responsible for γ-catenin increase following β-catenin down-regulation in HCC cells. First, we sought any change in mRNA expression of γ-catenin gene (*JUP*) after β-catenin KD in Hep3B cells. As observed *in vivo*, we did not observe any change in *JUP* expression despite an increase in γ-catenin protein (Figure 4*A*). Next, on the basis of *in vivo* observations that γ-catenin increase in β-catenin KO livers was associated with increased serine and threonine phosphorylation of γ-catenin, we asked whether such posttranslational modification could, in fact, stabilize γ-catenin *in vitro.* We treated Hep3B cells with OA, a well-known inhibitor of serine/threonine phosphatases [50,51]. Treatment of Hep3B cells for 3 hours with OA led to an increase in total γ-catenin protein levels further supporting the role of serine/threonine phosphorylation in its stabilization (Figure 4*B*).

To address which specific serine/threonine kinases may be responsible for γ-catenin stabilization in Hep3B cells after β-catenin KD, we used six different inhibitors with specific activities. As described in Materials and Methods section, around 45 hours after transfection of Hep3B cells with β-catenin or control siRNA, the cells were treated with the inhibitors: H-89 (inhibits PKA, CaM kinase II, PKC and casein kinase I); PKG inhibitor (inhibits PKG and PKA); bisindolylmaleimide I (PKC inhibitor); KN-93 (CaM kinase II inhibitor only); ML-7 (inhibits myosin light chain kinase) and staurosporine (broad range). We compared the extent of increase of γ-catenin upon β-catenin KD following treatment with these inhibitors as assessed by densitometric analysis. While γ-catenin continued to increase around nine-fold after β-catenin KD in Hep3B cells when treated with DMSO, ML-7, or KN-93 and around six-fold with BIS and staurosporine, only 1.75-fold increase was evident after treatment with H-89 (Figure 4*C*). No impact on γ-catenin was evident with water or PKG inhibitor treatment.

To further substantiate the role of PKA in γ-catenin stabilization after β-catenin KD, we next studied response to 3 hours of H-89 at low (150 nM) and high (20 μM) concentration on γ-catenin expression at 21 and 45 hours after β-catenin or control siRNA transfection. Both doses are within the range of specifically inhibiting PKA since concentration of only 30 μM or more impacts other serine/threonine kinases such as CaM kinase II, myosin light chain kinase, and casein kinase I [52]. At a 24-hour time point, there was a two- to three-fold induction in γ-catenin after β-catenin KD that was decreased by H-89 treatment at 150 nM or 20 μM by around 20% (Figure 4*D*). However, at 48 hours, there was a decrease in γ-catenin by around 40% with 150 nM and by 50% with 20 μM of H-89 treatment for 3 hours (Figure 4*D*). Lastly, using bioinformatics approach, we queried human γ-catenin protein sequence for potential PKA kinase substrate motifs using the Human Protein Reference Database PhosphoMotif Finder [53]. This led to the identification of 23 putative PKA phosphorylation sites in both the human and mouse junctional plakoglobin proteins, supporting the possibility of PKA phosphorylation of γ-catenin (Table 2).

Table 2. Putative PKA Phosphorylation Sites on Human and Mouse Junctional Plakoglobin.

	Sequence	Position	Motif	Location
1	KVT	12–14	[R/K]X[pS/pT]	N terminus
2	SSK	38–40	[pS/pT]X[R/K]	N terminus
3	TLK	54–56	[pS/pT]X[R/K]	N terminus
	KKT	56–58	[R/K]X[pS/pT]	
	KKTT	56–59	KXX[pS/pT]	
	KKTT	56–59	[R/K][R/K]X[pS/pT]	
	KKTTT	56–60	KXXX[pS/pT]	
4	TAR	79–81	[pS/pT]X[R/K]	N terminus
5	SKK	170–172	[pS/pT]X[R/K]	Arm domain
	KKEAS	171–175	KXXX[pS/pT]	
	KEAS	172–175	KXX[pS/pT]	
6	SRR	175–177	[pS/pT]X[R/K]	Arm domain
7	TAR	201–203	[pS/pT]X[R/K]	Arm domain
	RCT	203–205	[R/K]X[pS/pT]	
8	RMLS	233–236	RXXpS	Arm domain
9	RNYS	320–323	RXXpS	C terminus
10	KLLWT	326–330	KXXX[pS/pT]	C terminus
11	TSR	331–333	[pS/pT]X[R/K]	C terminus
12	KVLS	336–339	KXX[pS/pT]	C terminus
13	SNK	343–345	[pS/pT]X[R/K]	C terminus
14	KHLT	359–362	KXX[pS/pT]	C terminus
	KHLTS	359–363	KXXX[pS/pT]	
15	SPR	365–367	[pS/pT]X[R/K]	C terminus
16	TLR	375–377	[pS/pT]X[R/K]	C terminus
	RNLS	377–380	RXXpS	
17	KNKT	424–427	KXX[pS/pT]	C terminus
	KTLVT	426–430	KXXX[pS/pT]	
18	KDDIT	448–452	KXXX[pS/pT]	C terminus
19	TSR	463–465	[pS/pT]X[R/K]	C terminus
20	SVR	475–477	[pS/pT]X[R/K]	C terminus
21	KAT	499–501	[R/K]X[pS/pT]	C terminus
22	RIS	651–653	RXpS	C terminus
	RIS	651–653	[R/K]X[pS/pT]	
	KRVS	662–665	KXX[pS/pT]	
	KRVS	662–665	[R/K][R/K]X[pS/pT]	
	RVS	663–665	RXpS	
	RVS	663–665	[R/K]X[pS/pT]	
23	TYR	700–702	[pS/pT]X[R/K]	C terminus

siRNA-Mediated Double KD of β- and γ-Catenins In Vitro *in Hep3B Cells*

To try and effectively tease out the individual roles of β- and γ-catenins in HCC cells and to address biologic implications of γ-catenin stabilization following β-catenin KD, we investigated the feasibility of double KD (dKD) of β- and/or γ-catenin in addition to single KD (sKD) in Hep3B cells. WB analysis of siRNA-treated Hep3B cells at 24, 48, and 72 hours shows that the KD of these proteins is visible by 24 hours after transfection and persists to at least 72 hours after transfection (Figure 5*A*). Importantly, the increase in γ-catenin with β-catenin KD is apparent at all time points (Figure 5*A*). Additionally, the Hep3B cells transfected with single or double siRNAs appear healthy and viable at all time points tested and lacked any obvious changes in cell morphology (data not shown).

γ-Catenin KD in Hep3B Cells Leads to Increase in β-Catenin Expression

To address if analogous to β-catenin sKD γ-catenin sKD would alter β-catenin levels, we assessed the impact of γ-catenin KD in

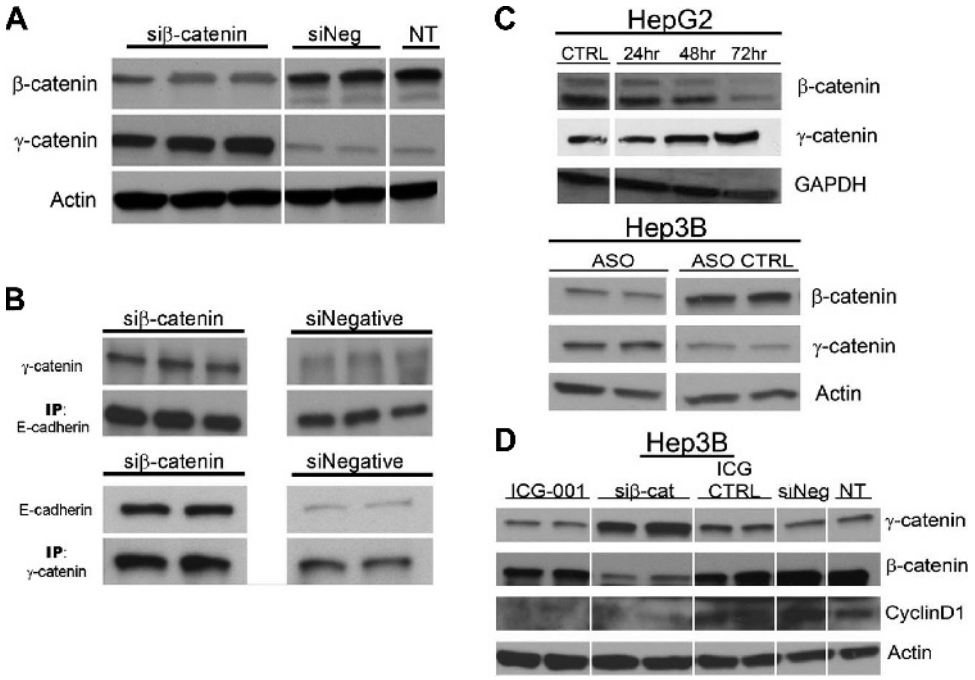

Figure 3. sKD of β-catenin protein accurately replicates conditions of β-catenin KO *in vivo*. (A) siRNA (siβ-catenin) induces efficient KD of β-catenin (92 kDa) in Hep3B cells and leads to an increase of γ-catenin (83 kDa) protein levels. (B) Whole-cell lysates from siβ-catenin and siNegative-treated Hep3B cells were immunoprecipitated with anti–E-cadherin or anti–γ-catenin antibodies. WB performed for γ-catenin (upper panel) and E-cadherin (120 kDa; lower panel) shows differential co-precipitation with sKD of β-catenin. (C) Hep3B and HepG2 cells treated with ASO to β-catenin show a decrease in β-catenin protein and subsequent increase in γ-catenin by WB. Both the WT and truncated forms of β-catenin in HepG2 cells show decrease with ASO. (D) KD of β-catenin activity using small molecule inhibitor ICG-001 does not change the protein levels of β- or γ-catenin, despite the decrease in β-catenin activity indicated by a decrease in its target cyclin D1 (37 kDa).

Hep3B cells. Interestingly, we observe an increase in β-catenin protein, especially at 24 and 48 hours of γ-catenin siRNA transfection (Figure 5*A*). This is in agreement with the recent cardiomyocyte-specific γ-catenin KO mice, which show an increase in β-catenin protein levels. However, the literature is mixed on the role of this β-catenin pool [54,55]. One study shows that the increase in β-catenin with γ-catenin loss is localized to the AJ [54], while another report suggests this increase to be nuclear since it led to an increase in β-catenin target gene expression [55]. Therefore, we looked at the AJ composition with γ-catenin sKD to see if there are any changes in β-catenin–E-cadherin association. We observe no apparent changes in their association in γ-catenin sKD (Figure 5*B*), indicating that the increase in β-catenin is most likely occurring in the nuclear/cytoplasmic and thus signaling pool of β-catenin in HCC cells.

γ-Catenin Does Not Compensate for β-Catenin–Mediated Wnt Signaling In Vitro*, while γ-Catenin KD Increases β-Catenin/TCF Reporter Activity in HCC Cells*

We have reported previously a lack of nuclear γ-catenin in hepatocyte-specific β-catenin KO mice even at time of β-catenin–dependent hepatocyte proliferation such as 72 hours after partial hepatectomy, indicating that γ-catenin was not compensating for nuclear β-catenin signaling *in vivo* [31]. To test it *in vitro*, we used a TOPflash luciferase reporter to assess TCF-dependent signaling of β- and γ-catenins. As expected, sKD of β-catenin leads to decreased TOPflash activity (Figure 5*C*). A dKD of β- and γ-catenins shows a decrease in Wnt signaling, but there is no additional impact of γ-catenin KD on the TOPflash reporter activity (Figure 5*C*), suggesting that γ-catenin does not contribute to Wnt signaling and therefore cannot compensate for β-catenin loss in the Wnt signaling cascade in HCC cells.

Interestingly, there is a significant increase in TOPflash activity with γ-catenin sKD (Figure 5*C*). This was in agreement with the increase in β-catenin levels in the non–E-cadherin–bound fraction, after γ-catenin sKD, and further supports that the increased β-catenin after γ-catenin sKD is nuclear (Figure 5*B*). To directly address this biologically, we examined [^{3}H]thymidine incorporation with dKD and sKD of β- and γ-catenins as a measure of cell proliferation. As expected, and in agreement with TOPflash reporter activity, we observe a decrease in thymidine incorporation after sKD of β-catenin or dKD of both catenins. However, also in concordance with TOPflash results, there is an increase in proliferation with γ-catenin sKD, *albeit* at 72 hours and not 48 hours after KD, which is most likely due to physiological delay in transactivation of cell cycle–related target genes governing this event (Figure 5*D*).

dKD of β- and γ-Catenins In Vitro *Decreased E-Cadherin Levels*

Since γ-catenin associated with E-cadherin in the absence of β-catenin, and β-catenin–E-cadherin association prevents degradation of E-cadherin by masking the PEST domain in E-cadherin, we next asked if γ-catenin–E-cadherin association could have similar function in E-cadherin stability. Hep3B cells subjected to sKD and dKD of catenins were assayed for E-cadherin levels by WB. While comparable levels of E-cadherin protein were observed in control siRNA-transfected Hep3B cells, and after sKD

of β-catenin or γ-catenin, a notable decrease was observed in dKD (Figure 5*E*). These data suggest that just like β-catenin, γ-catenin can bind effectively to E-cadherin and prevent its degradation in HCC cells.

dKD of β- and γ-Catenins In Vitro *Increases Rate of Migration of HCC Cells in Wound Closure Assay*

We next queried if γ-catenin up-regulation after β-catenin KD in HCC cells is conserving cell adhesions comparable to β-catenin. Hep3B cells after sKD or dKD were used for scratch wound assay to measure cell migration as described in Materials and Methods section. We observe that while with an sKD of either β-catenin or γ-catenin alone leads to no significant change in the percentage of wound closure after 24 hours, the dKD of both catenins significantly enhances wound closure at this time when compared to Hep3B cells treated with a negative control siRNA (Figure 6, *A* and *B*). These data indicate that the dKD of β- and γ-catenins is detrimental to overall cell adhesion thus increasing cell migration, while sKD of β-catenin is adequately compensated by γ-catenin and sKD of γ-catenin has no impact by AJ since E-cadherin–β-catenin association remains unaltered as shown earlier (Figure 5*B*).

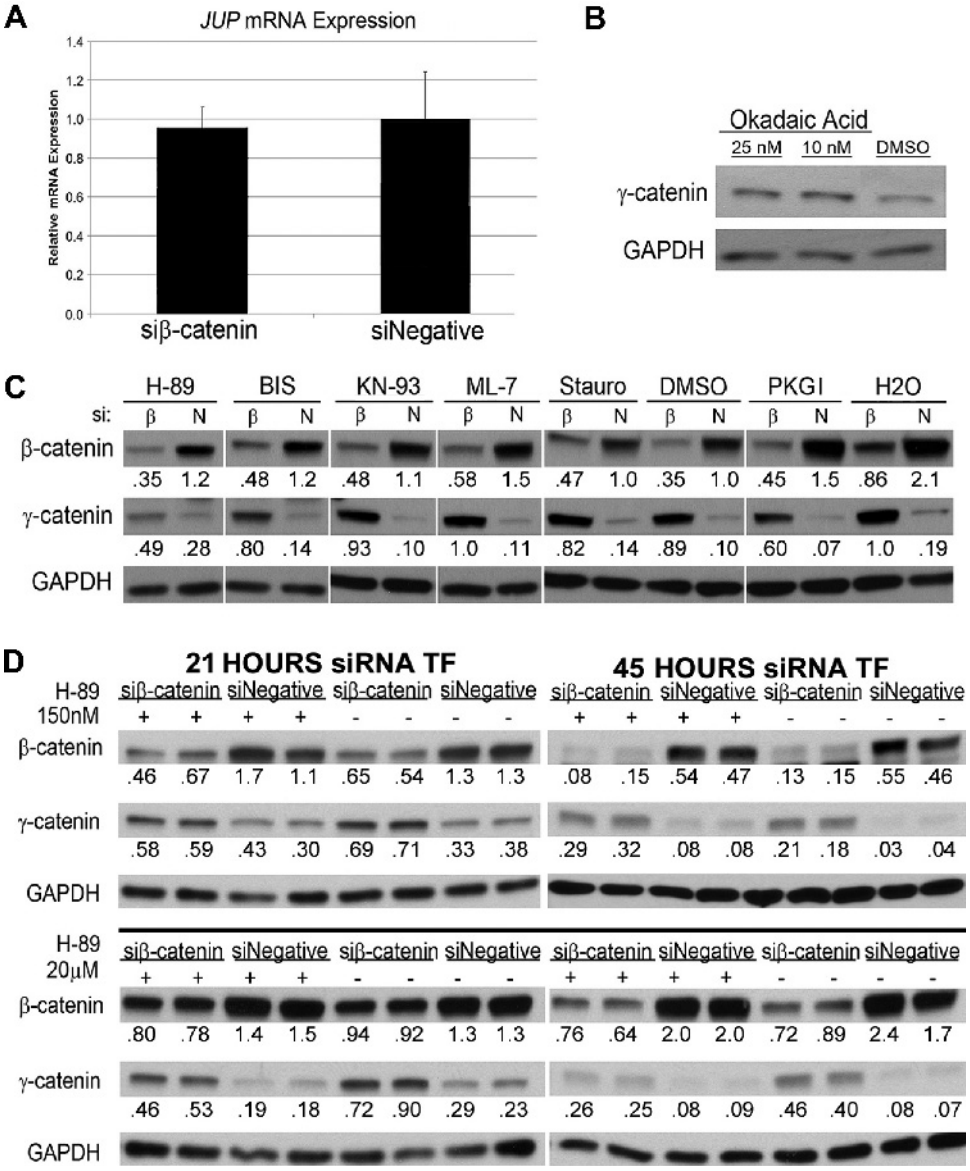

Figure 4. Mechanism of γ-catenin stabilization after sKD of β-catenin. (A) Real-time PCR for γ-catenin gene (*JUP*) and *GAPDH* reference gene shows insignificant difference in average mRNA expression (±SD) in siβ-catenin *versus* siNegative Hep3B-treated cells at 48-hour KD ($n = 3$). (B) Treatment of Hep3B cells for 3 hours with 10 or 25 nM OA, a known serine/threonine phosphatase inhibitor, results in increase in γ-catenin (83 kDa) as shown in a representative WB. (C) Treatment of Hep3B cells with various serine/threonine kinase inhibitors for 3 hours after 45 hours of transfection with control or β-catenin siRNA reveals a decrease in stabilization of γ-catenin after H-89 (PKA inhibitor). The numbers below the WB represent integrated optical density normalized to GAPDH (loading control) for the respective lane. (D) Treatment of Hep3B cells with H-89 at 150 nM and 20 μM for 3 hours after 21 or 45 hours of transfection with siβ-catenin or siNegative reveals a dose- and time-dependent decrease in extent of γ-catenin stabilization. The numbers below the WB represent integrated optical density normalized to GAPDH (loading control) for the respective lane.

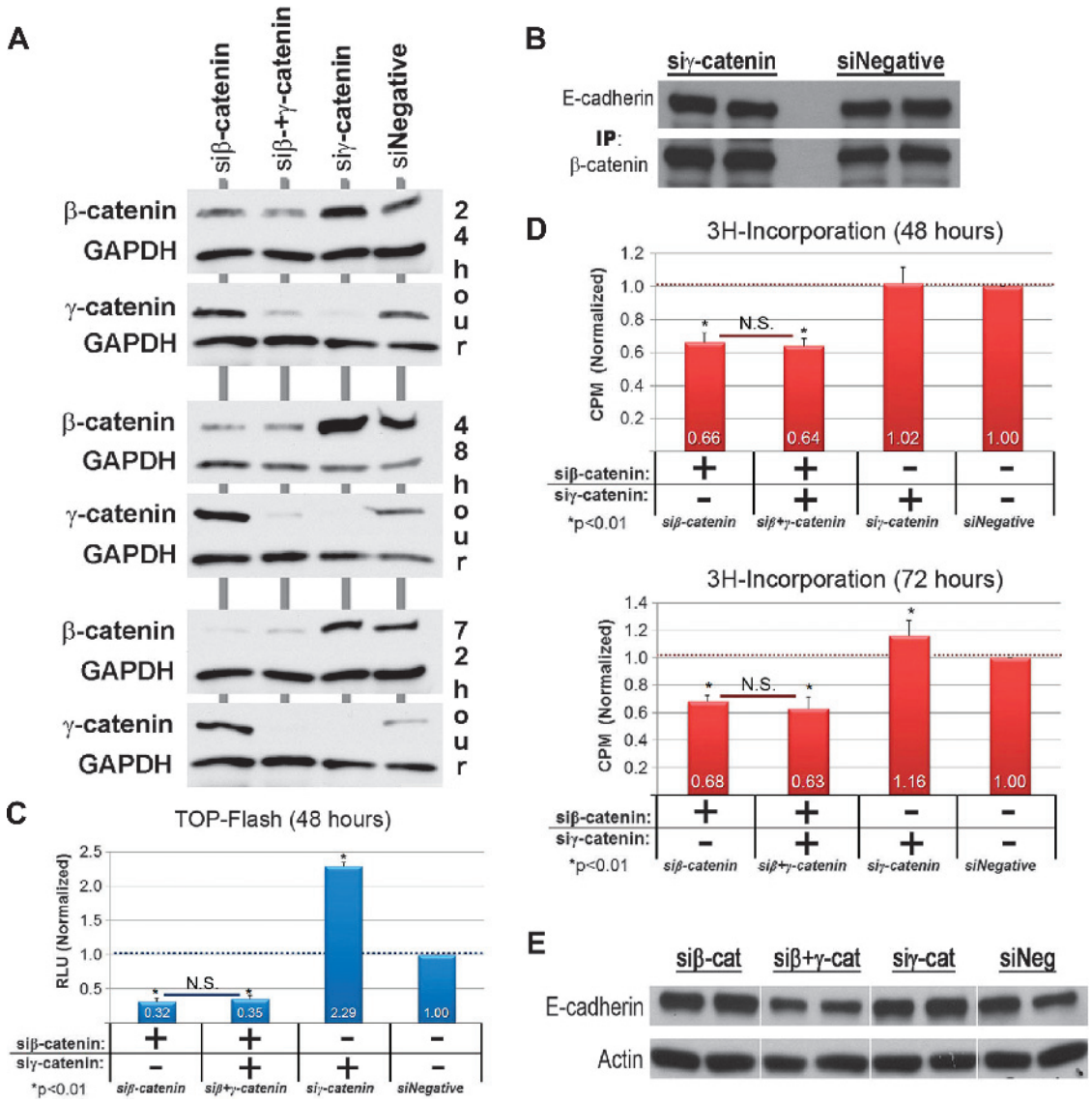

Figure 5. sKD and dKD of β- and γ-catenins with siRNA in Hep3B, a human HCC cell line, and impact on Wnt signaling, DNA synthesis, and E-cadherin. (A) Representative WBs showing a time course of sKD and dKD of β- and γ-catenins using siRNA in Hep3B cells. KD begins at 24 hours and persists for 72 hours after transfection. (B) Whole-cell lysates from siγ-catenin and siNegative-treated Hep3B cells were immunoprecipitated with an anti–β-catenin antibody. WB shows no changes in β-catenin's association with AJ protein E-cadherin. (C) Wnt reporter (TOPflash) activity is significantly decreased after sKD of β-catenin and dKD; however, there are insignificant differences between these two groups. A significant increase of TOPflash activity is observed after sKD of γ-catenin at 48 hours ($P < .01$; ±SD; asterisk indicates significance compared to siNegative; NS, not significant). (D) Upper panel: Thymidine incorporation (counts per minute) for sKD and dKD shows a significant but comparable decrease in DNA synthesis with sKD of β-catenin and dKD compared to siNegative. No change in DNA synthesis with sKD of γ-catenin at 48-hour KD was observed. Lower panel: Thymidine incorporation decreased comparably and significantly for sKD of β-catenin and dKD at 72 hours as well. A significant increase in DNA synthesis was observed with sKD of γ-catenin at 72-hour KD ($P < .01$; ±SD; asterisk indicates significance compared to siNegative; NS, not significant). (E) Representative WBs from lysates of Hep3B cells show a modest decrease in E-cadherin after dKD at 48 hours, while comparably higher levels are observed in sKD and siNegative conditions.

dKD of β- and γ-Catenins in Hep3B Cells Negatively Affects Cell-Cell Adhesion

To more directly test the functionality of γ-catenin at cell-cell adhesions after β-catenin KD, we next employed a CAFCA to compare the overall strength of cell-cell adhesions after sKD and dKD using Hep3B cells as described in Materials and Methods section. siRNA-treated Hep3B cells were plated on an untreated monolayer of Hep3B cells and subjected to a centrifugal force of 375*g*. At this force, we observed a significant decrease in cell-cell adhesion as measured by an increase in the percentage of cells lost, only with the dKD of β- and γ-catenins, when compared to control or sKD (Figure 6*C*).

To further validate cadherin-mediated cell-cell adhesions specifically (as in [37]), we used a hanging drop assay, where cells are cultured in suspension. After 24 hours in suspension, all the treatments formed colonies of relatively similar size; however, the dKD colonies appeared smaller and more asymmetric than others (Figure 6*D*, *upper panel*). To confirm that we were measuring calcium-dependent or cadherin-mediated adhesion, the single-cell suspension of Hep3B

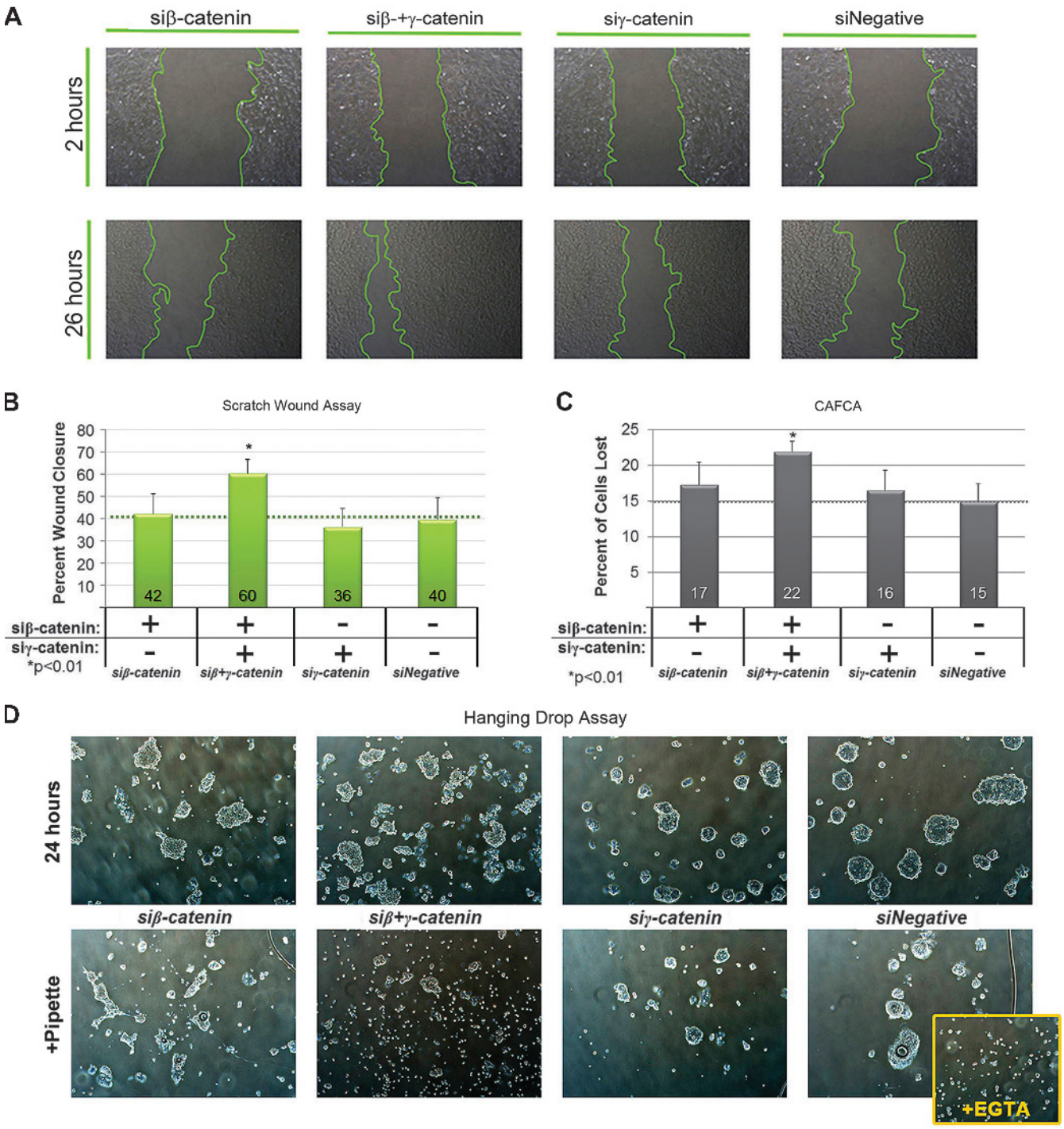

Figure 6. dKD of β- and γ-catenins affects cell migration and cell-cell adhesion *in vitro*. (A) Representative images of wound closure at 24 hours after initiation of the wound and 48 hours after transfection with various siRNAs. (B) Scratch wound assay for sKD and dKD Hep3B cells shows a significant increase in wound closure percentage for dKD of β- and γ-catenins only ($P < .01$; ±SD; asterisk indicates significance compared to siNegative). (C) CAFCA with sKD and dKD Hep3B cells shows a significant decrease in heterotypic cell-cell adhesion with dKD of β- and γ-catenins only ($P < .01$; ±SD; asterisk indicates significance compared to siNegative) as measured by increase in percentage of cells that de-adhere from the monolayer after centrifugation at 375*g* for 10 minutes. (D) Hanging drop assay shows that at 24 hours after drop formation (72-hour transfection) the colonies formed appear similar in size, though the dKD and sKD of β-catenin colonies appear to be less symmetric than the sKD γ-catenin and siNegative colonies. After pipetting, the dKD cells dissociate the most, indicating weaker homotypic cell-cell adhesions. Addition of EGTA, a calcium chelator, to siNegative-treated cells was used as a control to show that colonies formed were calcium-dependent or cadherin-based cell-cell adhesion.

cells transfected with control siRNA was also cultured in the presence of EGTA, a calcium chelator, which led to the absence of any colony formation after 24 hours, indicating that indeed these colonies required calcium to make new cell-cell adhesions (Figure 6*D*). When the colonies of hanging drop cultures were triturated, only the dKD dissociated readily to single-cell suspension, indicating weaker homotypic intercellular adhesions (Figure 6*D*).

Together, the data support maintenance of AJ by γ-catenin upon β-catenin loss and that concomitant decrease of β- and γ-catenins will be detrimental to intercellular adhesion and effectiveness of AJ.

Discussion

Anti–β-catenin therapies for treatment of various cancers including HCC are on the horizon [13,56]. In the current study, we addressed the consequences of altering β-catenin expression on the cadherin-based cell-cell adhesions and Wnt signaling due to ensuing compensations to determine if anti–β-catenin therapies may have unintended negative consequences on the progression of HCC. The observation that γ-catenin is upregulated after β-catenin loss both *in vitro* and *in vivo* and that γ-catenin can function at the AJ and as a part of Wnt signaling while being a natural component of desmosomes required extensive analysis to address both normal and acquired functions of γ-catenin in these circumstances.

It was important to initially address the influence of γ-catenin changes with β-catenin loss on the desmosomes, especially since the trafficking of γ-catenin to the AJ is controlled posttranscriptionally [31,41,46]. Additionally, disruptions in desmosomes have been shown to play a role in cancer progression [20,57,58], and thus compensation by γ-catenin at AJ may come at the expense of desmosomal integrity, which may have unintended negative side effects upon β-catenin therapeutic targeting in HCC. We have previously shown using a hepatocyte-specific β-catenin KO mouse that γ-catenin is increased and compensating for β-catenin loss at AJ by complexing with E-cadherin [31]. We now show that such compensation does not have any functional consequences on desmosomal structure in the liver. This was confirmed in multiple ways, including the observation that the γ-catenin/E-cadherin/Pkp3 cytoplasmic complex, which has been shown to be important for desmosomal assembly [48], was unchanged in KO mice. We also show that the structure of desmosomes was not affected *in vivo.* We did, however, see an increase in Pkp3 but are unable to explain the significance of this increase at this time. We speculate that Pkp3 increase after β-catenin loss may be more directly related to the changes in Wnt signaling than changes in AJ since we did not see changes in Pkp3 localization through fractionation or co-precipitation studies and still remains under scrutiny in our laboratory.

To fully investigate the impact of β-catenin loss on cell-cell adhesions, we employed an *in vitro* model of catenin KD. Having an *in vitro* model gives us the ability to modulate the two catenins singly or in combination and determine the impact through the simple readouts. Hep3B cells lent themselves well for such a model, although the role and regulation of γ-catenin upon β-catenin KD was also evident in other cell lines such as HepG2 cells and by other modalities of KD such as ASOs.

Adhesion of Hep3B cells to another monolayer of Hep3B cells through CAFCA was modestly and significantly decreased upon dKD of β- and γ-catenins. We ascribe the modest changes in the CAFCA to junctional crosstalk and compensation, which we have previously observed in the *in vivo* KO of β-catenin [31,34] and have also been seen in the *in vivo* models of γ-catenin KD [55,59]. There are known nodes of crosstalk between AJ and desmosomes [60], AJ and tight junctions [61], along with AJ and gap junctions [62]. We propose that such redundancies enable maintenance of cell-cell adhesions in epithelial cells and hence be permissive to therapies that may affect a junctional protein like β-catenin.

To tease out the exact roles of β- and γ-catenins on desmosomes and AJ, we used more specific assays for isolating cadherin-mediated adhesions. The hanging drop assay confirmed that cadherin-mediated adhesion is greatly decreased with the dKD of β- and γ-catenins but not with either sKD. This indicates that at least one of these catenins is necessary for the proper maintenance of cadherin-mediated junctions, corroborating the data put forth previously [37]. These data may also be influenced by the fact that we see an overall decrease in E-cadherin levels in our dKD Hep3B cells, which would reduce the pool of E-cadherin available for dimerization and assembly of AJ and would most likely reduce the overall number of AJ as well. The decrease in E-cadherin levels may be a result of the lack of catenins available to traffic E-cadherin to the membrane. β-Catenin interacts with E-cadherin to mask the PEST domain of E-cadherin, preventing its recognition by the proteasome [63]. Thus, on the basis of the similarities of β- and γ-catenin interactions with E-cadherin [15], we assume that γ-catenin allows for E-cadherin stabilization by masking its PEST domain, at least *in vitro*, and after acute β-catenin KD. Indeed, various studies have postulated that the interactions of β-catenin and γ-catenin with E-cadherin are indistinguishable. Choi and others showed that the crystal structures of β-catenin and γ-catenin with E-cadherin were nearly identical, although the dissociation constant of β-catenin binding to E-cadherin was nearly twice compared to γ-catenin (41 and 85 nM, respectively) [15]. This may suggest some minor differences in the interactions between the two catenins and E-cadherin. However, our data do indicate that at least one of the catenins is necessary for the maintenance of cadherin-mediated junctions and for steady-state E-cadherin expression.

Our study also demonstrates that decreasing β-catenin levels blocks canonical Wnt signaling, which is the major contributor toward HCC cell proliferation and survival. γ-Catenin increase with β-catenin KD is unable to compensate for β-catenin signaling, as shown by TOPflash assay. Indeed, in our previous studies, we failed to detect any increase in nuclear γ-catenin in β-catenin KO livers even at times of ongoing proliferation [31]. Similarly, despite γ-catenin increase in β-catenin KO livers, several liver-specific targets of β-catenin such as glutamine synthetase and cytochrome *P*450s 2E1 and 1A2 continued to be significantly downregulated in KO [14].

γ-Catenin increase secondary to β-catenin KD does not worsen HCC cell phenotype by promoting tumor cell proliferation, migration, or Wnt activation. Others have published studies indicating that an increase in γ-catenin leads to enhancement of metastasis through genomic instability and migration [64]. However, we accredit the lack of detrimental phenotypes seen with γ-catenin increase with sKD of β-catenin to a strictly compensatory function of γ-catenin *in lieu* of β-catenin at the AJ. Thus, γ-catenin appears to have a protective effect when β-catenin levels are decreased, acting as a tumor suppressor. However, on its own, γ-catenin appears to have rather mixed effects. While, on the one hand, sKD of γ-catenin did not negatively impact cell-cell adhesions or migration, we did observe an increase in proliferation preceded by an increase in β-catenin signaling. Therefore, in our studies we observed that γ-catenin does not explicitly act as an oncogene or tumor suppressor but that its role in HCC cells may be closely linked to that of

β-catenin, although additional studies like generation of hepatocyte-specific γ-catenin KO would be necessary. Our data suggest that only combined inhibition of β-catenin and γ-catenin leads to more migration of cells and perhaps may induce local invasion and metastasis, which is a concept also shown previously in a clinical study, where it was not the overall levels of catenins that determined the prognosis of HCC, but instead it correlated better with combined expression of catenins and E-cadherin. Specifically, the authors observed poor prognosis and survival rate in HCC patients exhibiting decrease in both γ-catenin and E-cadherin and not a decrease in γ-catenin alone [21].

We next addressed the molecular basis of γ-catenin increase following β-catenin loss. In our previous work, we identified enhanced serine/threonine and not tyrosine phosphorylation of γ-catenin [31]. This mechanism was also verified *in vitro* when OA, a known serine/threonine phosphatase inhibitor, induced γ-catenin levels in Hep3B cells [23,25,50,51]. γ-Catenin is indeed known to undergo serine/threonine phosphorylation [41]. Since cytoplasmic but not insoluble membrane-associated pool of γ-catenin showed serine and threonine phosphorylation, it suggests that phosphorylation may prevent γ-catenin degradation during cytoplasmic trafficking [41]. In our studies, on the basis of the overlap of activities of various kinase inhibitors used and observed dose-dependent response, it appears that PKA is the candidate serine/threonine kinase responsible for phosphorylating γ-catenin to induce its stabilization in the absence of β-catenin. Although additional mutagenesis studies will be essential, *in silico* analysis identified 23 putative PKA substrate motifs located throughout γ-catenin protein. Future studies will address PKA-dependent phosphorylation for specific residues in γ-catenin that are critical for its stabilization especially after β-catenin KD.

Preclinical β-catenin inhibitors being investigated can be broadly categorized into two classes: 1) those that block the nuclear β-catenin without impacting the total levels of β-catenin (such as ICG-001 and pegylated interferon-α2a) [8,11] and 2) those that suppress β-catenin gene and/or protein expression such as ASO or other indirectly acting agents [10,65–68]. Results from ASO, siRNA, and ICG-001 studies indicate that it is the absolute levels of β-catenin and not a decrease in β-catenin's transactivational activity that provides an impetus for γ-catenin stabilization and that the compensation by γ-catenin is at the AJ only and the functions of β-catenin as a part of the Wnt pathway remain unfulfilled by γ-catenin. This suggests that there may exist a catenin-sensing mechanism in a cell, which monitors the levels of catenins especially at junctions and allows for compensation for these proteins by others through relatively prompt post-translational modifications. We propose that PKA may be such a sensor, which stabilizes γ-catenin and is also known to phosphorylate β-catenin at serine 552 and 675 to induce its activation [69]. Whether PKA normally phosphorylates membrane-bound β-catenin is not known, although the two effector serine/threonine sites are in close proximity to tyrosine 654 and 670, which are the sites phosphorylated by receptor tyrosine kinases known to deregulate E-cadherin–β-catenin complex at AJ [70,71]. We therefore propose that when β-catenin levels diminish, PKA is unable to activate β-catenin, which now switches substrates to phosphorylate γ-catenin instead and this induces γ-catenin stabilization to at least fulfill the role of β-catenin at the AJ. While this hypothesis needs further experimental proof, it does demonstrates the feasibility of β-catenin–decreasing agents as therapies for HCC, provided γ-catenin stabilization factors such as PKA are spared for adequate compensation at junctions to prevent untoward effects on tumor cell migration, invasion, and metastasis.

Acknowledgments

The authors thank Jelena Grahovac for her technical help with the CAFCA, attachment assay, and scratch wound assay in the laboratory of Dr Alan Wells at the University of Pittsburgh. The authors also thank Wei Yang for his technical help with the inhibitor assays.

References

[1] El-Serag HB (2004). Hepatocellular carcinoma: recent trends in the United States. *Gastroenterology* **127**, S27–S34.
[2] Parkin DM, Bray F, Ferlay J, and Pisani P (2005). Global cancer statistics, 2002. *CA Cancer J Clin* **55**, 74–108.
[3] Waly Raphael S, Yangde Z, and Yuxiang C (2012). Hepatocellular carcinoma: focus on different aspects of management. *ISRN Oncol* **2012**, 421673.
[4] Kondo Y, Kanai Y, Sakamoto M, Genda T, Mizokami M, Ueda R, and Hirohashi S (1999). Beta-catenin accumulation and mutation of exon 3 of the beta-catenin gene in hepatocellular carcinoma. *Jpn J Cancer Res* **90**, 1301–1309.
[5] Legoix P, Bluteau O, Bayer J, Perret C, Balabaud C, Belghiti J, Franco D, Thomas G, Laurent-Puig P, and Zucman-Rossi J (1999). Beta-catenin mutations in hepatocellular carcinoma correlate with a low rate of loss of heterozygosity. *Oncogene* **18**, 4044–4046.
[6] Wong CM, Fan ST, and Ng IO (2001). Beta-Catenin mutation and overexpression in hepatocellular carcinoma: clinicopathologic and prognostic significance. *Cancer* **92**, 136–145.
[7] de La Coste A, Romagnolo B, Billuart P, Renard CA, Buendia MA, Soubrane O, Fabre M, Chelly J, Beldjord C, Kahn A, et al. (1998). Somatic mutations of the β-catenin gene are frequent in mouse and human hepatocellular carcinomas. *Proc Natl Acad Sci USA* **95**, 8847–8851.
[8] Emami KH, Nguyen C, Ma H, Kim DH, Jeong KW, Eguchi M, Moon RT, Teo JL, Kim HY, Moon SH, et al. (2004). A small molecule inhibitor of β-catenin/CREB-binding protein transcription [corrected]. *Proc Natl Acad Sci USA* **101**, 12682–12687.
[9] Stock P, Monga D, Tan X, Micsenyi A, Loizos N, and Monga SP (2007). Platelet-derived growth factor receptor-α: a novel therapeutic target in human hepatocellular cancer. *Mol Cancer Ther* **6**, 1932–1941.
[10] Behari J, Zeng G, Otruba W, Thompson MD, Muller P, Micsenyi A, Sekhon SS, Leoni L, and Monga SP (2007). R-Etodolac decreases β-catenin levels along with survival and proliferation of hepatoma cells. *J Hepatol* **46**, 849–857.
[11] Thompson MD, Dar MJ, and Monga SP (2011). Pegylated interferon alpha targets Wnt signaling by inducing nuclear export of β-catenin. *J Hepatol* **54**, 506–512.
[12] Clevers H and Nusse R (2012). Wnt/β-catenin signaling and disease. *Cell* **149**, 1192–1205.
[13] Nejak-Bowen KN and Monga SP (2011). Beta-catenin signaling, liver regeneration and hepatocellular cancer: sorting the good from the bad. *Semin Cancer Biol* **21**, 44–58.
[14] Tan X, Behari J, Cieply B, Michalopoulos GK, and Monga SP (2006). Conditional deletion of beta-catenin reveals its role in liver growth and regeneration. *Gastroenterology* **131**, 1561–1572.
[15] Choi HJ, Gross JC, Pokutta S, and Weis WI (2009). Interactions of plakoglobin and β-catenin with desmosomal cadherins: basis of selective exclusion of α- and β-catenin from desmosomes. *J Biol Chem* **284**, 31776–31788.
[16] Maeda O, Usami N, Kondo M, Takahashi M, Goto H, Shimokata K, Kusugami K, and Sekido Y (2004). Plakoglobin (γ-catenin) has TCF/LEF family-dependent transcriptional activity in β-catenin-deficient cell line. *Oncogene* **23**, 964–972.
[17] Kim YM, Ma H, Oehler VG, Gang EJ, Nguyen C, Masiello D, Liu H, Zhao Y, Radich J, and Kahn M (2011). The gamma catenin/CBP complex maintains survivin transcription in β-catenin deficient/depleted cancer cells. *Curr Cancer Drug Targets* **11**, 213–225.
[18] Anderson JM (1996). Leaky junctions and cholestasis: a tight correlation. *Gastroenterology* **110**, 1662–1665.
[19] Sakisaka S, Kawaguchi T, Taniguchi E, Hanada S, Sasatomi K, Koga H, Harada M, Kimura R, Sata M, Sawada N, et al. (2001). Alterations in tight junctions differ between primary biliary cirrhosis and primary sclerosing cholangitis. *Hepatology* **33**, 1460–1468.
[20] Cao Y, Chang H, Li L, Cheng RC, and Fan XN (2007). Alteration of adhesion molecule expression and cellular polarity in hepatocellular carcinoma. *Histopathology* **51**, 528–538.

[21] Zhai B, Yan HX, Liu SQ, Chen L, Wu MC, and Wang HY (2008). Reduced expression of E-cadherin/catenin complex in hepatocellular carcinomas. *World J Gastroenterol* **14**, 5665–5673.

[22] Zhang XF, Tan X, Zeng G, Misse A, Singh S, Kim Y, Klaunig JE, and Monga SP (2010). Conditional β-catenin loss in mice promotes chemical hepatocarcinogenesis: role of oxidative stress and platelet-derived growth factor receptor α/phosphoinositide 3-kinase signaling. *Hepatology* **52**, 954–965.

[23] Rubiolo JA, Lopez-Alonso H, Vega FV, Vieytes MR, and Botana LM (2011). Okadaic acid and dinophysis toxin 2 have differential toxicological effects in hepatic cell lines inducing cell cycle arrest, at G0/G1 or G2/M with aberrant mitosis depending on the cell line. *Arch Toxicol* **85**, 1541–1550.

[24] Gesty-Palmer D, Chen M, Reiter E, Ahn S, Nelson CD, Wang S, Eckhardt AE, Cowan CL, Spurney RF, Luttrell LM, et al. (2006). Distinct β-arrestin- and G protein-dependent pathways for parathyroid hormone receptor-stimulated ERK1/2 activation. *J Biol Chem* **281**, 10856–10864.

[25] Hirooka K, Kourennyi DE, and Barnes S (2000). Calcium channel activation facilitated by nitric oxide in retinal ganglion cells. *J Neurophysiol* **83**, 198–206.

[26] Yu P, Han W, Villar VA, Li H, Arnaldo FB, Concepcion GP, Felder RA, Quinn MT, and Jose PA (2011). Dopamine D1 receptor-mediated inhibition of NADPH oxidase activity in human kidney cells occurs via protein kinase A-protein kinase C cross talk. *Free Radic Biol Med* **50**, 832–840.

[27] Breitwieser GE and Gama L (2001). Calcium-sensing receptor activation induces intracellular calcium oscillations. *Am J Physiol Cell Physiol* **280**, C1412–C1421.

[28] Citi S (1992). Protein kinase inhibitors prevent junction dissociation induced by low extracellular calcium in MDCK epithelial cells. *J Cell Biol* **117**, 169–178.

[29] Kelps KA, Turchan-Cholewo J, Hascup ER, Taylor TL, Gash DM, Gerhardt GA, and Bradley LH (2011). Evaluation of the physical and *in vitro* protective activity of three synthetic peptides derived from the pro- and mature GDNF sequence. *Neuropeptides* **45**, 213–218.

[30] Simcha I, Shtutman M, Salomon D, Zhurinsky J, Sadot E, Geiger B, and Ben-Ze'ev A (1998). Differential nuclear translocation and transactivation potential of β-catenin and plakoglobin. *J Cell Biol* **141**, 1433–1448.

[31] Wickline ED, Awuah PK, Behari J, Ross M, Stolz DB, and Monga SP (2011). Hepatocyte γ-catenin compensates for conditionally deleted β-catenin at adherens junctions. *J Hepatol* **55**, 1256–1262.

[32] Monga SP, Mars WM, Pediaditakis P, Bell A, Mule K, Bowen WC, Wang X, Zarnegar R, and Michalopoulos GK (2002). Hepatocyte growth factor induces Wnt-independent nuclear translocation of β-catenin after Met-β-catenin dissociation in hepatocytes. *Cancer Res* **62**, 2064–2071.

[33] Wack KE, Ross MA, Zegarra V, Sysko LR, Watkins SC, and Stolz DB (2001). Sinusoidal ultrastructure evaluated during the revascularization of regenerating rat liver. *Hepatology* **33**, 363–378.

[34] Behari J, Yeh TH, Krauland L, Otruba W, Cieply B, Hauth B, Apte U, Wu T, Evans R, and Monga SP (2010). Liver-specific β-catenin knockout mice exhibit defective bile acid and cholesterol homeostasis and increased susceptibility to diet-induced steatohepatitis. *Am J Pathol* **176**, 744–753.

[35] Awuah PK, Rhieu BH, Singh S, Misse A, and Monga SP (2012). β-Catenin loss in hepatocytes promotes hepatocellular cancer after diethylnitrosamine and phenobarbital administration to mice. *PLoS One* **7**, e39771.

[36] Zou L, Jaramillo M, Whaley D, Wells A, Panchapakesa V, Das T, and Roy P (2007). Profilin-1 is a negative regulator of mammary carcinoma aggressiveness. *Br J Cancer* **97**, 1361–1371.

[37] Fukunaga Y, Liu H, Shimizu M, Komiya S, Kawasuji M, and Nagafuchi A (2005). Defining the roles of β-catenin and plakoglobin in cell-cell adhesion: isolation of β-catenin/plakoglobin-deficient F9 cells. *Cell Struct Funct* **30**, 25–34.

[38] Sekine S, Ogawa R, and Kanai Y (2011). Hepatomas with activating *Ctnnb1* mutations in '*Ctnnb1*-deficient' livers: a tricky aspect of a conditional knockout mouse model. *Carcinogenesis* **32**, 622–628.

[39] Thompson MD, Wickline ED, Bowen WB, Lu A, Singh S, Misse A, and Monga SP (2011). Spontaneous repopulation of β-catenin null livers with β-catenin-positive hepatocytes after chronic murine liver injury. *Hepatology* **54**, 1333–1343.

[40] Miravet S, Piedra J, Castano J, Raurell I, Franci C, Dunach M, and Garcia de Herreros A (2003). Tyrosine phosphorylation of plakoglobin causes contrary effects on its association with desmosomes and adherens junction components and modulates β-catenin-mediated transcription. *Mol Cell Biol* **23**, 7391–7402.

[41] Pasdar M, Li Z, and Chlumecky V (1995). Plakoglobin: kinetics of synthesis, phosphorylation, stability, and interactions with desmoglein and E-cadherin. *Cell Motil Cytoskeleton* **32**, 258–272.

[42] Sacco PA, McGranahan TM, Wheelock MJ, and Johnson KR (1995). Identification of plakoglobin domains required for association with N-cadherin and α-catenin. *J Biol Chem* **270**, 20201–20206.

[43] Troyanovsky R, Chitaev N, and Troyanovsky S (1996). Cadherin binding sites of plakoglobin: localization, specificity and role in targeting to adhering junctions. *J Cell Sci* **109**, 3069–3078.

[44] Wahl J, Sacco P, McGranahan-Sadler T, Sauppe L, Wheelock M, and Johnson K (1996). Plakoglobin domains that define its association with the desmosomal cadherins and the classical cadherins: identification of unique and shared domains. *J Cell Sci* **109**, 1143–1154.

[45] Zhou J, Qu J, Yi XP, Graber K, Huber L, Wang X, Gerdes AM, and Li F (2007). Upregulation of γ-catenin compensates for the loss of β-catenin in adult cardiomyocytes. *Am J Physiol Heart Circ Physiol* **292**, H270–H276.

[46] Kowalczyk AP, Palka HL, Luu HH, Nilles LA, Anderson JE, Wheelock MJ, and Green KJ (1994). Posttranslational regulation of plakoglobin expression. Influence of the desmosomal cadherins on plakoglobin metabolic stability. *J Biol Chem* **269**, 31214–31223.

[47] Vinken M, Papeleu P, Snykers S, De Rop E, Henkens T, Chipman JK, Rogiers V, and Vanhaecke T (2006). Involvement of cell junctions in hepatocyte culture functionality. *Crit Rev Toxicol* **36**, 299–318.

[48] Gosavi P, Kundu ST, Khapare N, Sehgal L, Karkhanis MS, and Dalal SN (2011). E-cadherin and plakoglobin recruit plakophilin3 to the cell border to initiate desmosome assembly. *Cell Mol Life Sci* **68**, 1439–1454.

[49] Bonne S, van Hengel J, Nollet F, Kools P, and van Roy F (1999). Plakophilin-3, a novel armadillo-like protein present in nuclei and desmosomes of epithelial cells. *J Cell Sci* **112**(pt 14), 2265–2276.

[50] Dounay AB and Forsyth CJ (2002). Okadaic acid: the archetypal serine/threonine protein phosphatase inhibitor. *Curr Med Chem* **9**, 1939–1980.

[51] Haystead TA, Sim AT, Carling D, Honnor RC, Tsukitani Y, Cohen P, and Hardie DG (1989). Effects of the tumour promoter okadaic acid on intracellular protein phosphorylation and metabolism. *Nature* **337**, 78–81.

[52] Chijiwa T, Mishima A, Hagiwara M, Sano M, Hayashi K, Inoue T, Naito K, Toshioka T, and Hidaka H (1990). Inhibition of forskolin-induced neurite outgrowth and protein phosphorylation by a newly synthesized selective inhibitor of cyclic AMP-dependent protein kinase, *N*-[2-(*p*-bromocinnamylamino)ethyl]-5-isoquinolinesulfonamide (H-89), of PC12D pheochromocytoma cells. *J Biol Chem* **265**, 5267–5272.

[53] Amanchy R, Periaswamy B, Mathivanan S, Reddy R, Tattikota SG, and Pandey A (2007). A curated compendium of phosphorylation motifs. *Nat Biotechnol* **25**, 285–286.

[54] Li D, Liu Y, Maruyama M, Zhu W, Chen H, Zhang W, Reuter S, Lin SF, Haneline LS, Field LJ, et al. (2011). Restrictive loss of plakoglobin in cardiomyocytes leads to arrhythmogenic cardiomyopathy. *Hum Mol Genet* **20**, 4582–4596.

[55] Li J, Swope D, Raess N, Cheng L, Muller EJ, and Radice GL (2011). Cardiac tissue-restricted deletion of plakoglobin results in progressive cardiomyopathy and activation of β-catenin signaling. *Mol Cell Biol* **31**, 1134–1144.

[56] Dahmani R, Just PA, and Perret C (2011). The Wnt/β-catenin pathway as a therapeutic target in human hepatocellular carcinoma. *Clin Res Hepatol Gastroenterol* **35**, 709–713.

[57] Brooke MA, Nitoiu D, and Kelsell DP (2012). Cell-cell connectivity: desmosomes and disease. *J Pathol* **226**, 158–171.

[58] Chidgey M and Dawson C (2007). Desmosomes: a role in cancer? *Br J Cancer* **96**, 1783–1787.

[59] Swope D, Cheng L, Gao E, Li J, and Radice GL (2012). Loss of cadherin-binding proteins β-catenin and plakoglobin in the heart leads to gap junction remodeling and arrhythmogenesis. *Mol Cell Biol* **32**, 1056–1067.

[60] Lewis JE, Wahl JK, Sass KM, Jensen PJ, Johnson KR, and Wheelock MJ (1997). Cross-talk between adherens junctions and desmosomes depends on plakoglobin. *J Cell Biol* **136**, 919–934.

[61] Konopka G, Tekiela J, Iverson M, Wells C, and Duncan SA (2007). Junctional adhesion molecule-A is critical for the formation of pseudocanaliculi and modulates E-cadherin expression in hepatic cells. *J Biol Chem* **282**, 28137–28148.

[62] Yoshida M, Ohkusa T, Nakashima T, Takanari H, Yano M, Takemura G, Honjo H, Kodama I, Mizukami Y, and Matsuzaki M (2011). Alterations in adhesion junction precede gap junction remodelling during the development of heart failure in cardiomyopathic hamsters. *Cardiovasc Res* **92**, 95–105.

[63] Hinck L, Nathke IS, Papkoff J, and Nelson WJ (1994). Dynamics of cadherin/catenin complex formation: novel protein interactions and pathways of complex assembly. *J Cell Biol* **125**, 1327–1340.

[64] Pan H, Gao F, Papageorgis P, Abdolmaleky HM, Faller DV, and Thiagalingam S (2007). Aberrant activation of γ-catenin promotes genomic instability and oncogenic effects during tumor progression. *Cancer Biol Ther* **6**, 1638–1643.

[65] Huang WS, Wang JP, Wang T, Fang JY, Lan P, and Ma JP (2007). ShRNA-mediated gene silencing of β-catenin inhibits growth of human colon cancer cells. *World J Gastroenterol* **13**, 6581–6587.

[66] Liyan W, Xun S, and Xiangwei M (2011). Effect of β-catenin siRNA on proliferation and apoptosis of hepatoma cell line SMMC-7721 and HepG-2. *Hepatogastroenterology* **58**, 1757–1764.

[67] Zeng G, Apte U, Cieply B, Singh S, and Monga SP (2007). siRNA-mediated β-catenin knockdown in human hepatoma cells results in decreased growth and survival. *Neoplasia* **9**, 951–959.

[68] Zhao JH, Luo Y, Jiang YG, He DL, and Wu CT (2011). Knockdown of β-catenin through shRNA cause a reversal of EMT and metastatic phenotypes induced by HIF-1α. *Cancer Invest* **29**, 377–382.

[69] Taurin S, Sandbo N, Qin Y, Browning D, and Dulin NO (2006). Phosphorylation of β-catenin by cyclic AMP-dependent protein kinase. *J Biol Chem* **281**, 9971–9976.

[70] Piedra J, Martinez D, Castano J, Miravet S, Dunach M, and de Herreros AG (2001). Regulation of β-catenin structure and activity by tyrosine phosphorylation. *J Biol Chem* **276**, 20436–20443.

[71] Zeng G, Apte U, Micsenyi A, Bell A, and Monga SP (2006). Tyrosine residues 654 and 670 in β-catenin are crucial in regulation of Met–β-catenin interactions. *Exp Cell Res* **312**, 3620–3630.

Table W1. List of Antibodies.

Protein	Antibody Species	kDa	WB Dilution	IF Dilution	IP Dilution	Company	Product Number
β-Actin	Mouse	42	1:2500	X	X	Millipore	MAB1501
β-Catenin	Mouse	92	1:1000	X	X	BD	610154
β-Catenin	Rabbit	92	X	1:150	X	Santa Cruz Biotechnology	sc-7199
β-Catenin	Goat	X	X	X	1:50	Santa Cruz Biotechnology	sc-1496 AC
Cyclin D1	Mouse	37	1:200	X	X	Santa Cruz Biotechnology	sc-20044
Dsc2	Goat	110	1:200	X	X	Santa Cruz Biotechnology	sc-34311
Dsg1	Rabbit	150/160	1:200	X	X	Santa Cruz Biotechnology	sc-20114
Dsg2	Rabbit	59–150	1:200	X	X	Santa Cruz Biotechnology	sc-20115
Dsg3	Goat	108/130/100/80/75/55	1:200	X	X	Santa Cruz Biotechnology	sc-14867
Dsg4	Goat	99/115	1:200	X	X	Santa Cruz Biotechnology	sc-28069
DPI/II	Rabbit	210/250	1:200	X	X	Santa Cruz Biotechnology	sc-33555
E-cadherin	Rabbit	120	X	X	1:50	Santa Cruz Biotechnology	sc-7870
E-cadherin	Mouse	120	1:1000	X	X	BD	610182
γ-Catenin	Rabbit	80–87	1:1000	1:50	1:100	Cell Signaling Technology	2309
γ-Catenin	Goat	80–87	1:200	1:50	X	Santa Cruz Biotechnology	sc-30997
γ-Catenin	Goat	80–87	1:200	1:50	X	Santa Cruz Biotechnology	sc-30996
GAPDH	Rabbit	37	1:1000	X	X	Santa Cruz Biotechnology	sc-25778
Pkp2	Goat	100	1:200	X	X	Santa Cruz Biotechnology	sc-18977
Pkp3	Mouse	87	1:200	X	X	Santa Cruz Biotechnology	sc-166655
Pkp3	Rabbit	87	1:500	X	X	Abcam	ab109441

GAPDH indicates glyceraldehyde-3-phosphate dehydrogenase.

Table W2. Real-Time PCR Primer Sequences.

Gene	Species	Direction	Sequence	Reference
JUP	Human	Forward	5′-AAG GTG CTA TCC GTG TGT CC-3′	[71]
JUP	Human	Reverse	5′-GAC GTT GAC GTC ATC CAC AC-3′	[71]
GAPDH	Human	Forward	5′-TGC ACC ACC AAC TGC TTA GC-3′	[72]
GAPDH	Human	Reverse	5′-GGC ATG GAC TGT GGT CAT GAG-3′	[72]